Calcium Oxide Nanoparticles for Chromium (VI) Adsorption: Green Synthesis and Adsorption Studies

Dandy Firmansyah Rifli¹, Maulana¹, Suhendra² & Syukrya Ningsih^{1*}

¹Departmen Department of Chemistry, UIN Sulthan Thaha Saifuddin, Jambi, Indonesia
² Departmen Department of Geographic Information Science, UIN Sulthan Thaha
Saifuddin, Jambi, Indonesia
*Email: syukryaningsih@uinjambi.ac.id

Abstract. The purpose of this study was to synthesize and characterize calcium oxide nanoparticles from Lokan shell using the top-down method with thermal decomposition and then applied to the adsorption of Cr (IV) metal ions. The results of the analysis of the CaO content of the Lokan shell were determined to be 97.513% by XRF analysis. The study of surface morphology and functional groups of calcium oxide as an adsorbent was carried out using SEM, XRD, and FTIR. Adsorption efficiency and capacity with variations in concentration and contact time were studied from the results of AAS analysis, showing an optimum adsorption capacity of 4.606 mg/g. In this study, CaO was identified as an environmentally friendly and effective adsorbent for removing Cr(IV) metal from water samples.

Keywords: Adsorption capacity; Chromium; Lokan shell; Nanoparticles.

1 Introduction

Wastewater regulations are designed to reduce human and environmental exposure to pesticides, heavy metals, and other hazardous chemicals (Saravanan et al., 2021). The types and concentrations of contaminants found in water bodies are of increasing concern (Singh, Anil, et al., 2022; Singh, Naik, et al., 2022). For example, higher concentrations of chromium in aquatic environments, especially drinking water, can cause a number of diseases including eye irritation, kidney damage, skin irritation, respiratory cancer, and tooth discoloration (Azeez et al., 2021; Huang et al., 2019). The International Agency for Research on Cancer (IARC) classifies the hexavalent form as a Group I carcinogen. According to WHO recommendations, the maximum acceptable level of Cr in drinking water is 50 mg/L (Rada et al., 2021; Tabatabaei et al., 2020). In addition, exposure to Cr(VI) can cause death in humans at lethal doses between 50 and 150 mg/kg (Shi et al., 2020). Cr(VI) is a chemical used in various industries, including electroplating, metal alloys, tanning, textiles, and papermaking.

To remove Cr(VI) ions from water bodies, various removal techniques have been used, including chemical precipitation, absorption, coagulation-flocculation, and

ion exchange (Choudhary & Paul, 2018; Tabatabaei et al., 2020). Due to their large surface area and sorption capacity, nano-sized adsorbents are commonly used to remove Cr(VI) from aqueous solutions via sorption (Adebayo et al., 2020; Mahapatra et al., 2022). To date, it has been reported that cheap and environmentally friendly adsorbents, such as rice husks, coconut fibers, banana peel pulp, and various other agricultural biomasses, can treat metal-containing water (Daneshvar et al., 2019; Dhanya et al., 2020; Singh, Anil, et al., 2022; Zhang et al., 2024).

Currently, shellfish commodities have been widely utilized by society and industry, especially Lokan shellfish (*Geloina erosa*) (Abdal-hay et al., 2023; Imaduddin & Samik, 2023). However, as a result of this increased activity, there is an impact in the form of processed waste that is rarely utilized so that it has the potential to pollute the environment. Based on the results of previous research, it shows that as much as 67.7% of the CaCO₃ content is contained in Lokan shells (Adji et al., 2023). The unique properties of calcium make research related to this material continue to be carried out until now. Nanoparticle materials have various surface functions and are promising adsorbents. Therefore, the aim of this research is to develop a recycling process of shell waste into calcium oxide nanoparticles through an environmentally friendly method to remove toxic pollutants such as heavy metals and other contaminants.

2 Methodology

2.1 Materials

The materials used in this study were Lokan shell (*Geloina erosa*) obtained from the community around Teluk Majelis Village, East Tanjung Jabung Regency, Jambi Province, Indonesia and potassium dichromate (K₂Cr₂O₇) purchased from Sigma.

2.2 Adsorbent characterization

Lokan shell content was analyzed using X-ray Fluorescence (Rigaku Supermini-200). Adsorbent characterization was analyzed using Field Emission Scanning Electron Microscope (SEM) analysis (Thermo Apreo 2), to obtain particle shape or morphology. X-ray Diffraction (XRD) type Shimadzu-7000 to analyze crystal size and crystal structure, and analysis of functional groups of adsorbent compounds using Fourier Transform Infrared Spectroscopy (FTIR) (Perkin Elmer Spectrum Two System L160000A).

2.3 Synthesis of calcium oxide adsorbent

Lokan shells were thoroughly cleaned and then dried in an oven at 50°C for 2 hours. Then, the shells were crushed using a ring mill until they reached a flour-like consistency. Next, the flour was sieved using a 200mesh sieve. To obtain calcium oxide nanoparticles, the Lokan shell flour was calcined at 800°C, 900°C, and 1000°C, for 4 hours. The resulting CaO nanoparticles were then further analyzed to determine their specific characteristics before application. The work steps in this study refer to research (Handayani & Syahputra, 2017) with some modifications.

2.4 Adsorption Study (Batch)

Cr(VI) stock solution (1000 mg/L) was prepared by dissolving $K_2Cr_2O_7$ in distilled water. Batch adsorption experiments were conducted by adding 0.1 g of adsorbent into 100 mL of Cr(VI) solution. The contact variation of adsorption parameters carried out was the time and concentration of Cr(VI), at time variations (50, 75, 100 and 125 minutes) and concentration variations (10, 20, 30 and 40 mg/L) then stirred using a magnetic stirrer at a speed of 150 rpm and a temperature of 25°C. The residue was filtered using filter paper (0.45 μ m) and the adsorbent solution was described using Atomic Absorption Spectrometry (AAS).

3 Results and Discussion

3.1 Adsorbent characterization

The results of XRF analysis show that Lokan shell has a very high calcium (Ca) content. Based on Table 1, the dominant element in Lokan shell flour is Ca with a level of 97.513%. In accordance with previous research (Wahyuningsih et al., 2018), P. maxima shell contains the highest CaO content, which is 93.53%.

The surface morphology of the samples was observed at 3000x, 8000x, and 15000x magnifications. The SEM test findings in Figure 1a show a heterogeneous morphology, but Figures 1b and 1c show a homogeneous morphology, as observed from microscopic analysis. Figure 1a, magnified at 8000x, depicts crystals arranged in layers which then aggregate to form larger sizes. The mechanism of the particles clumping together demonstrates the polycrystalline nature of the nano CaO derived from mussel flour. Meanwhile, Figures 1b and 1c show a more random surface morphology consisting of thin and uneven layers. Based on the SEM test results presented in Figure 1, it can be observed that nano CaO derived from Lokan shells exhibits a unique morphology characterized by calcite-type crystals.

	Element		(Oxides		
Compound	Conc.	Unit	Compound	Conc.	Unit	
Al	0,211	%	Al ₂ O ₃	0,349	%	
P	0,349	%	P_2O_5	0,683	%	
Cl	0,446	%	CaO	97,382	%	
Ca	97,513	%	TiO_2	0,013	%	
Ti	0,012	%	V_2O_5	0,003	%	
V	0,003	%	MnO	0,007	%	
Mn	0,008	%	Fe_2O_3	0,328	%	
Fe	0,35	%	ZnO	0,005	%	
Zn	0,006	%	SrO	0,649	%	
Br	0,006	%	ZrO_2	0,002	%	
Sr	0,841	%	Ag2O	0,215	%	
Zr	0,003	%	Cl	0,361	%	
Ag	0,254	%	Br	0,004	%	

Table 1 Chemical composition of Lokan shell

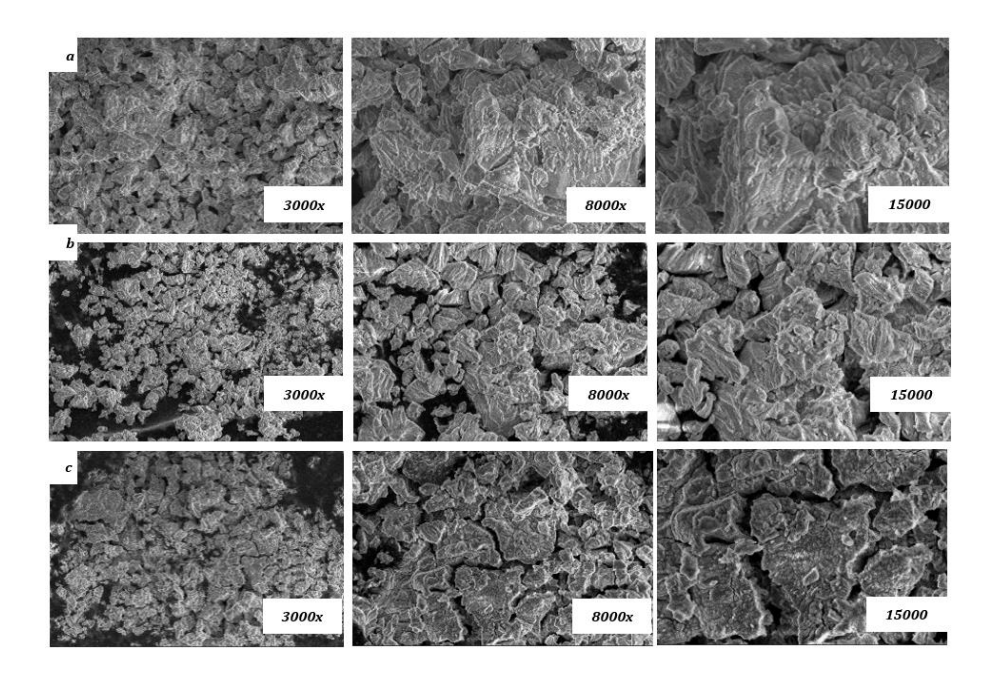


Figure 1 Surface morphology of Lokan shell ($Geloina\ erosa$) temperature calcination (a) 800°C (a), 900°C (b) and 1000°C (c)

According to (Liendo et al., 2022), calcite crystals exhibit rhombohedral, cubic scalenohedral, and prismatic morphologies. Previous research on the synthesis of nanocalcium from eggshells (Habte et al., 2019), the results found that calcium oxide nanoparticles have an almost spherical particle shape, as observed in SEM data. Each temperature produces different diffractograms as shown by the XRD

test results. The variation of the Lokan shell diffractogram peaks is due to the temperature difference during the calcination process. The XRD diffractogram results of Lokan shells with calcination treatment at 800° C, 900° C, and 1000° C are shown in Figure 2. At 800° C, the resulting peaks show the presence of CaCO₃, Ca(OH)₂ and CaO compounds, at certain angles, namely 2θ , 29.3° , 39.3° , 43.1° , 47.4° , and 48, 4° then Ca(OH)₂ peaks were observed at 2θ angles of 28.6° , 34.0° , 47.0° , and 50.8° and CaO peaks were observed at 2θ angles of 32.2° , 37.3° , 53.8° , 64.1° , and 67.3° . while at 900° C and 1000° C only two compounds were identified, namely Ca(OH)₂ and CaO.

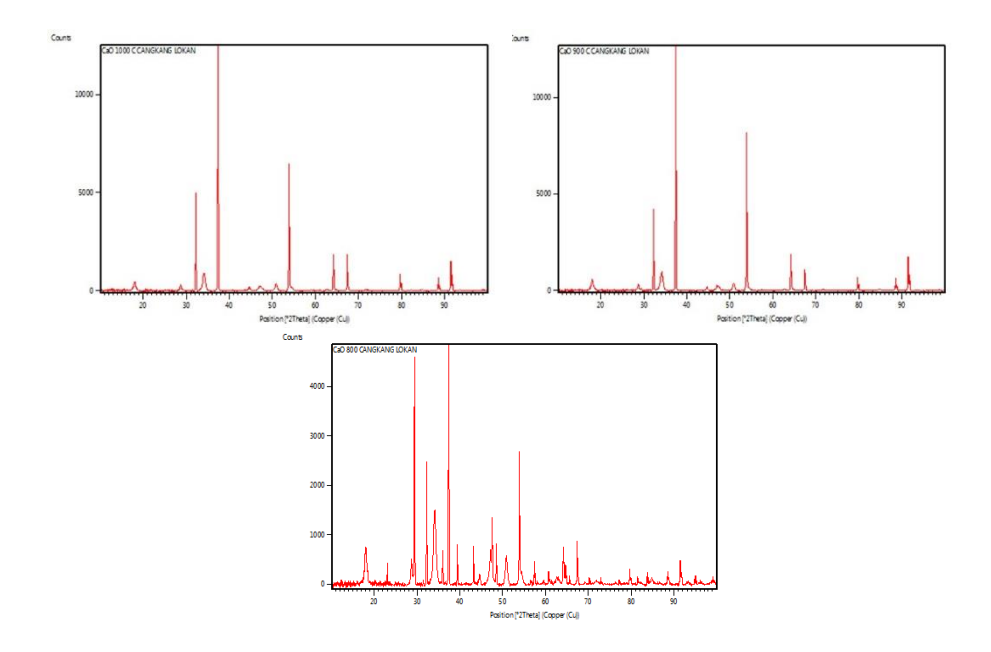


Figure 2 XRD spectra locan shell (*Geloina erosa*) temperature calcination 800° C (a) 900° C (b) and 1000° C (c).

The FTIR spectra of CaO adsorbent from Lokan shell calcined at 1000°C are depicted in Figure 3. Peaks corresponding to OH in Ca(OH)₂ were observed at two wave numbers, 3432.09 cm⁻¹ and 3642.86 cm⁻¹. Another band along 872.9 cm⁻¹ was found which represents the Ca-O bond. The FTIR peaks at 1633.07 cm⁻¹, 1479.33 cm⁻¹, and 1118.01 cm⁻¹ indicate the stretching vibrations of CO₃ 2-groups [36]. Therefore, the FTIR analysis indicates a complete calcination process in the Lokan shell modified to calcium oxide as Ca-O bonds.

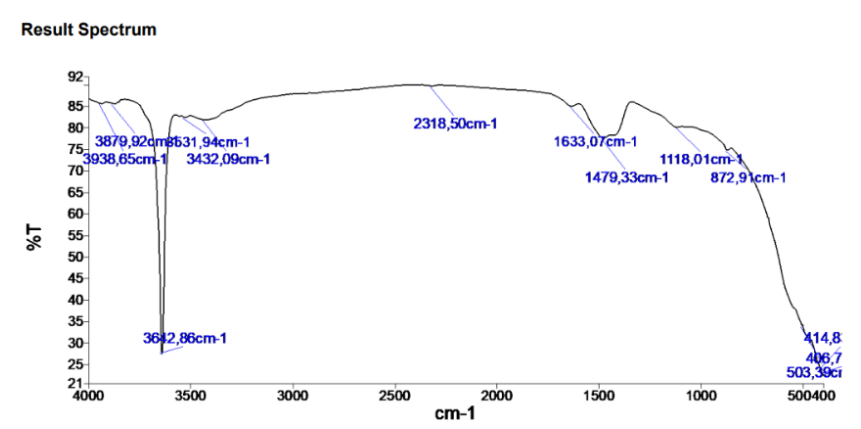


Figure 3 Spectra FTIR nano CaO calcination temperature 1000°C

Based on previous research, nano CaO undergoes rapid hydration when in contact with air. The O-C-O peak was observed at a wave number of 1479.33 cm⁻¹, indicating the presence of carbonation in calcium oxide nanoparticles (Shan et al., 2024). Observation of the O-C-O functional group at 1000°C provides evidence that the CaCO₃ compound decomposes into CaO during the calcination process (Habte et al., 2019).

3.2 Effect of contact time on adsorption

The level of adsorption efficiency of CaO nanoparticles from Lokan shell on Cr(VI) metal generally increased at the beginning of adsorption along with the increase of absorption contact time. This can be seen in Figure 4 where the graph pattern continues to increase at increasing contact time until the maximum at 125th minute with an efficiency value of 15.35%. Furthermore, the adsorption capacity with variations in contact time experiences a state that is directly proportional to that seen in Figure 4. A similar pattern is also obtained by research conducted by (Eddy et al., 2024) in general the adsorption process increases with increasing contact time. Furthermore, according to (Thakur et al., 2021) the adsorption capacity will increase with increasing contact time until it reaches an equilibrium state. On the other hand, active sites decrease and unfilled available sites are difficult to occupy due to repulsive forces between adsorbent and adsorbate molecules (Shan et al., 2024).

3.3 Effect of initial concentration on adsorption

The effect of initial concentration on the adsorption efficiency (%) of Cr(VI) metal from water media using CaO adsorbent was analyzed as in Figure 5, the maximum adsorption efficiency at a concentration of 20 ppm was 13.6%. While the effect of concentration variation on the adsorption capacity produced

increased along with the increase in Cr(VI) metal concentration, the maximum adsorption capacity value was at a concentration of 40 ppm at 4.403 mg/g.

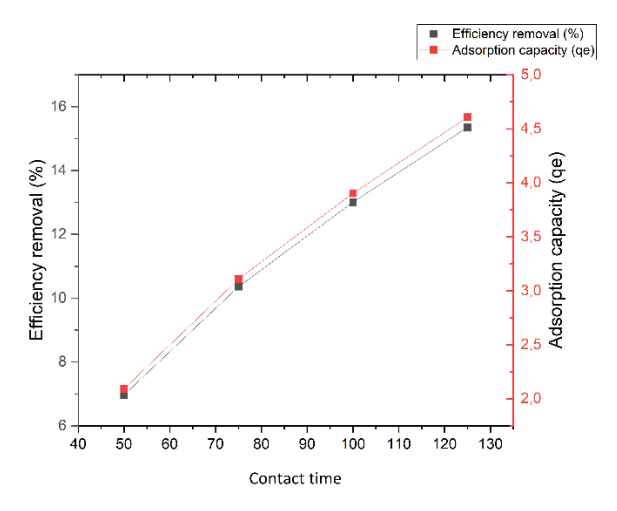


Figure 4 Effect of contact time on efficiency removal and adsorption capacity.

According to research conducted by (Kasirajan et al., 2022) the concentration factor plays an important role in the adsorption process, where the higher the concentration causes the adsorbent surface area to be saturated, resulting in the adsorbent being ineffective to use. Furthermore, the efficiency and capacity of adsorption show the opposite trend, this can occur because of the inverse relationship between adsorbent dose and absorption capacity (Shan et al., 2024).

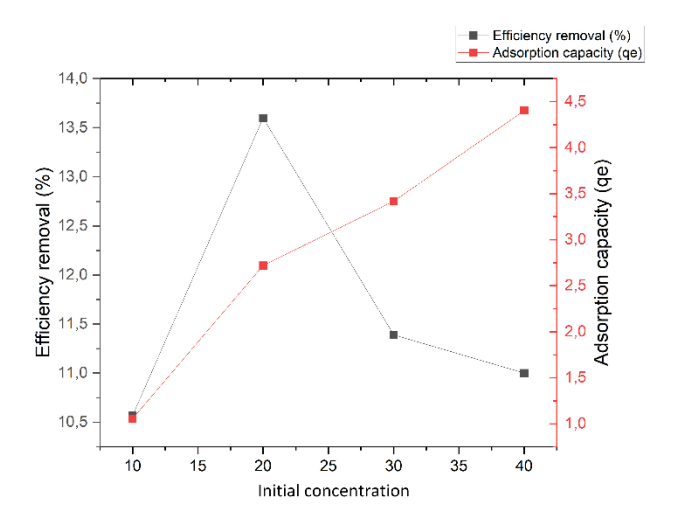


Figure 5 Effect of initial concentration on efficiency removal and adsorption capacity

4 Conclusion

Lokan shell calcined at 1000 0C has good adsorption capacity for Cr(VI) removal. The selected experimental conditions can be optimized to obtain the best results. The optimum operating condition of CaO to adsorb Cr(VI) efficiently is with a contact time of 125 minutes, using an adsorbent dose of 0.1 g in 100 mL Cr(VI) solution with an initial concentration of 30 mg/L. The adsorbent was characterized using SEM, XRD, and FTIR, which showed that the final content of the adsorbent was calcium oxide and the porous morphological structure indicated that metal ion adsorption could occur on the adsorbent.

5 Acknowledgement

This research supported by the Ministry of Religious Affairs Republic Indonesia. The authors fully acknowledge the technical support provided by the Integrated Laboratory of the State University of Padang, and the Advanced Physics Imaging Laboratory at National Research and Innovation Agency of The Republic of Indonesia.

References

- [1] Saravanan A, Senthil Kumar P, Jeevanantham S, Karishma S, Tajsabreen B, Yaashikaa PR, et al. *Effective water/wastewater treatment methodologies for toxic pollutants removal: Processes and applications towards sustainable development.* Chemosphere, 2021 Oct;280:130595.
- [2] Singh S, Naik TSSK, Anil AG, Khasnabis S, Nath B, U B, et al. *A novel CaO nanocomposite cross linked graphene oxide for Cr(VI) removal and sensing from wastewater.* Chemosphere. 2022 Aug;301:134714.
- [3] Singh S, Anil AG, Khasnabis S, Kumar V, Nath B, Adiga V, et al. Sustainable removal of Cr(VI) using graphene oxide-zinc oxide nanohybrid: Adsorption kinetics, isotherms and thermodynamics. Environ Res. 2022 Jan;203:111891.
- [4] Azeez NA, Dash SS, Gummadi SN, Deepa VS. *Nano-remediation of toxic heavy metal contamination: Hexavalent chromium [Cr(VI)]*. Chemosphere. 2021 Mar;266:129204.
- [5] Huang D, Liu C, Zhang C, Deng R, Wang R, Xue W, et al. *Cr(VI)* removal from aqueous solution using biochar modified with Mg/Allayered double hydroxide intercalated with ethylenediaminetetraacetic acid. Bioresour Technol. 2019 Mar;276:127–32.
- [6] Rada EC, Schiavon M, Torretta V. A regulatory strategy for the emission control of hexavalent chromium from waste-to-energy plants. J Clean Prod. 2021 Jan;278:123415.
- [7] Tabatabaei S, Forouzesh Rad B, Baghdadi M. Semicontinuous enhanced electroreduction of Cr(VI) in wastewater by cathode constructed of

- *copper rods coated with palladium nanoparticles followed by adsorption.* Chemosphere. 2020 Jul;251:126309.
- [8] Shi J, McGill WB, Chen N, Rutherford PM, Whitcombe TW, Zhang W. Formation and Immobilization of Cr(VI) Species in Long-Term Tannery Waste Contaminated Soils. Environ Sci Technol. 2020 Jun 16;54(12):7226–35.
- [9] Choudhary B, Paul D. *Isotherms, kinetics and thermodynamics of hexavalent chromium removal using biochar*. Journal of Environmental Chemical Engineering. 2018 Apr;6(2):2335–43.
- [10] Adebayo GB, Adegoke HI, Fauzeeyat S. Adsorption of Cr(VI) ions onto goethite, activated carbon and their composite: kinetic and thermodynamic studies. Appl Water Sci. 2020 Sep;10(9):213.
- [11] Mahapatra U, Manna AK, Chatterjee A. A critical evaluation of conventional kinetic and isotherm modeling for adsorptive removal of hexavalent chromium and methylene blue by natural rubber sludge-derived activated carbon and commercial activated carbon. Bioresour Technol. 2022 Jan;343:126135.
- [12] Daneshvar E, Zarrinmehr MJ, Kousha M, Hashtjin AM, Saratale GD, Maiti A, et al. *Hexavalent chromium removal from water by microalgal-based materials: Adsorption, desorption and recovery studies.* Bioresour Technol. 2019 Dec;293:122064.
- [13] Dhanya BS, Mishra A, Chandel AK, Verma ML. Development of sustainable approaches for converting the organic waste to bioenergy. Sci Total Environ. 2020 Jun 25;723:138109.
- [14] Zhang Y, Zhao W, Zhang X, Wang S. Highly efficient targeted adsorption and catalytic degradation of ciprofloxacin by a novel molecularly imprinted bimetallic MOFs catalyst for persulfate activation. Chemosphere. 2024 Jun;357:141894.
- [15] Abdal-hay A, Bartnikowski M, Blaudez F, Vaquette C, Hutmacher DW, Ivanovski S. *Unique uniformity of calcium phosphate nanoparticle distribution in polymer substrates for additive manufacturing*. Composites Part A: Applied Science and Manufacturing. 2023 Oct;173:107670.
- [16] Imaduddin M, Samik S. a riview: sintesis biodiesel dengan katalis heterogen dari cangkang hewan mollusca. ujc. 2023 Jan 17;12(1):12–9.
- [17] Adji NTL, Lucytasari SD, Suprihatin S. Sintesis dan karakterisasi nanokalsium oksida dari cangkang kerang hijau dengan metode presipitasi. Jurnal Teknik Kimia. 2023 Oct 31;18(1).
- [18] Handayani L, Syahputra F. Isolation and Identification Nanocalcium from Oyster Shell. Jurnal Pengolahan Hasil Perikanan Indonesia. 2017;
- [19] Wahyuningsih K, Jumeri J, Wagiman W. Optimization of Production Process of Nano-Calcium Oxide from Pinctada maxima Shell by Using Taguchi Method. Indones J Chem. 2018 Nov 26;19(2):356–67.
- [20] Liendo F, Arduino M, Deorsola FA, Bensaid S. Factors controlling and influencing polymorphism, morphology and size of calcium carbonate

- synthesized through the carbonation route: A review. Powder Technol. 2022 Jan;398:117050.
- [21] Habte L, Shiferaw N, Mulatu D, Thenepalli T, Chilakala R, Ahn J. Synthesis of Nano-Calcium Oxide from Waste Eggshell by Sol-Gel Method. Sustainability. 2019 Jun 7;11(11):3196.
- [22] Yulianti CH, Ediati R, Hartanto D, Purbaningtias TE, Chisaki Y, Jalil AA, et al. *Synthesis of caozno nanoparticles catalyst and its application in transesterification of refined palm oil*. Bull Chem React Eng Catal. 2014 Aug 1;9(2).
- [23] Shan GNM, Rafatullah M, Siddiqui MR, Kapoor RT, Qutob M. Calcium oxide from eggshell wastes for the removal of pharmaceutical emerging contaminant: Synthesis and adsorption studies. J Indian Chem Soc. 2024 Aug;101(8):101174.
- [24] Eddy NO, Oladede J, Eze IS, Garg R, Garg R, Paktin H. Synthesis and characterization of CaO nanoparticles from periwinkle shells for the treatment of tetracycline-contaminated water by adsorption and photocatalyzed degradation. Results in Engineering. 2024 Dec;24:103374.
- [25] Thakur S, Singh S, Pal B. *Time-dependent growth of CaO nano flowers from egg shells exhibit improved adsorption and catalytic activity*. Advanced Powder Technology. 2021 Sep;32(9):3288–96.
- [26] Kasirajan R, Bekele A, Girma E. Adsorption of lead (Pb-II) using CaO-NPs synthesized by solgel process from hen eggshell: Response surface methodology for modeling, optimization and kinetic studies. South African Journal of Chemical Engineering. 2022 Apr;40:209–29.